

Accelerated degradation modeling considering long-range dependence and unit-to-unit variability

Shi-Shun Chen ^{a, b}, Xiao-Yang Li ^{a, b, *}, Wenrui Xie ^c

^a School of Reliability and Systems Engineering, Beihang University, Beijing 100191, China

^b Science and Technology on Reliability and Environmental Engineering Laboratory, Beijing 100191, China

^c School of Mathematics, Jilin University, Changchun 130012, China

Highlights

- An improved non-Markovian ADT model is developed.
- The long-range dependence in the degradation process is described by the FBM.
- The unit-to-unit variability is considered in the degradation rate function.
- A novel statistical inference method is proposed based on the EM algorithm.

Abstract

Accelerated degradation testing (ADT) is an effective way to evaluate the reliability and lifetime of highly reliable products. Existing studies have shown that the degradation processes of some products are non-Markovian with long-range dependence due to the interaction with environments. Besides, the degradation processes of products from the same population generally vary from each other due to various uncertainties. These two aspects bring great difficulty for ADT modeling. In this paper, we propose an improved ADT model considering both long-range dependence and unit-to-unit variability. To be specific, fractional Brownian motion (FBM) is utilized to capture the long-range dependence in the degradation process. The unit-to-unit variability among multiple products is captured by a random variable in the degradation rate function. To ensure the accuracy of the parameter estimations, a novel statistical inference method based on expectation maximization (EM) algorithm is proposed, in which the maximization of the overall likelihood function is achieved. The effectiveness of the proposed method is fully verified by a simulation case and a microwave case. The results show that the proposed model is more suitable for ADT modeling and analysis than existing ADT models.

Keywords: Accelerated degradation testing; fractional Brownian motion; unit-to-unit variability; EM algorithm; long-range dependence.

1 Introduction

With the continuous progress of design and manufacturing technology, modern products tend to have extremely high reliability and long lifetime. At this point, accelerated degradation testing (ADT) is

always employed, in which degradation data are obtained under more severe stress conditions. By modeling ADT data, the lifetime and reliability of products under normal conditions can be extrapolated and the saving of cost and time can be achieved. In general, the commonly used degradation models for ADT modeling are stochastic process models. Charki et al. [1] carried out ADT on photovoltaic modules under three temperature and humidity levels and employed the Wiener process to inference its lifetime under normal conditions. Santini et al. [2] utilized the gamma process to model the threshold voltage degradation of a commercial SiC MOSFET at different temperature and gate voltage levels and assessed its reliability under normal conditions. Yan et al. [3] recorded the tensile force degradation of the flax fiber reinforced composite laminates under different temperature and humidity levels and evaluated its lifetime and reliability under normal conditions using the Tweedie exponential dispersion process. More related works on ADT modeling can be found in [4-6].

A reasonable description of the degradation process in ADT modeling is essential to ensure the credibility of the lifetime and reliability assessments. Most existing ADT models hold a general assumption that performance degradation is a memoryless Markovian process with independent increments. However, for real engineering products, such as batteries or blast furnace walls [7], degradation typically exhibits non-Markovian properties, i.e., the future degradation increment is influenced by the current or historical states. The root cause of this phenomenon can be attributed to the interaction with environments [8]. Since traditional Markovian models are completely memoryless, they fail to describe the degradation of such dynamic systems, leading to an imprecise lifetime and reliability assessments. Hence, building up an ADT model considering the non-Markovian degradation is essential for enabling more accurate extrapolation of lifetime and reliability.

To describe the non-Markovian property of a degradation process, some research introduced a state-dependent function to quantify the influence of the current state on the degradation rate and established different transformed stochastic processes. Giorgio et al. [10] established the transformed gamma process and derived the conditional distribution of the first passage time. Following this, Giorgio and Pulcini [9] further proposed the transformed Wiener process to describe the non-Markovian degradation process with possibly negative increments. Also, the transformed inverse Gaussian process [11] and the transformed exponential dispersion process [12] were presented and the corresponding parameter estimation methods based on the Bayesian framework were developed.

However, for the above transformed stochastic processes, it is difficult to choose a reasonable form of the state-dependent function without any prior knowledge. Besides, they only focus on the influence of the current state on the future degradation increment, which may not be sufficient for describing the long-range dependence of the entire degradation path. Different from the state-dependent function, fractional Brownian motion (FBM) is an effective mathematical tool for modeling non-Markovian stochastic processes with long-range dependence [13, 14]. In the FBM, the degree of long-range dependence can be simply quantified by the Hurst exponent. To this end, FBM has drawn much attention in degradation modeling [15]. Xi et al. [16] first introduced the FBM to capture the long-range dependence in the degradation process and predicted the remaining useful life (RUL) of a turbofan engine. They showed that the degradation model based on the FBM is more suitable to describe the degradation process than that based on the Wiener process. Afterward, Xi et al. [17] proposed an improved

degradation model by considering both the long-range dependence and unit-to-unit variability. Their results illustrated that catching the long-range dependence in the degradation data can improve the accuracy of the RUL prediction. Furthermore, Shao and Si [18] extended the degradation model based on the FBM by considering the measurement errors. Xi et al. [19] further developed a multivariate degradation model based on the FBM to describe multivariate stochastic degradation systems with long-range dependence. Besides, Zhang et al. [7] established a degradation model with long-range dependence and multiple modes, and presented a framework for automatic identification of the multiple modes in the degradation process. The above studies found that compared to the degradation models based on the Wiener process, the degradation models based on the FBM all obtained more accurate RUL predictions.

Although scholars have made much progress in degradation modeling based on the FBM, the above degradation models fail to quantify the effect of external stresses on performance degradation. Hence, they are incapable of assessing the reliability and lifetime of highly reliable products under limited time and resources. To solve this problem, in a recent study, Si et al [20] constructed an ADT model based on the FBM, thus quantifying the effect of external stresses on performance degradation and considering the long-range dependence in the degradation process. Their results indicated that the ADT model considering long-range dependence could get more accurate lifetime assessments than the Markovian ADT model.

Actually, the accuracy of lifetime extrapolation based on the ADT model depends not only on the reasonable description of the degradation process, but also on proper uncertainty quantification. In an ADT, we can observe that different items have different degradation paths, known as unit-to-unit variability. The unit-to-unit variability comes from the design, manufacturing and production stages of products [21]. For products with good consistency, ignoring unit-to-unit variability may have little effect on the accuracy of lifetime extrapolation. But for other products with poor consistency, unit-to-unit variability needs to be clearly distinguished and quantified, which otherwise provides little guidance for controlling these uncertainties and results in unreliable reliability and lifetime assessments in practical applications [22, 23]. Nonetheless, to the best of our knowledge, none of the existing ADT models with long-range dependence consider unit-to-unit variability.

Motivated by the above limitation, this paper constructs an improved non-Markovian ADT model considering both long-range dependence and unit-to-unit variability. Specifically, the long-range dependence is described by the FBM and unit-to-unit variability is quantified by a random variable in the degradation rate function. On this basis, a novel statistical inference method based on the EM algorithm is proposed to improve the accuracy of parameter estimations. The main contributions are summarized as follows:

- An improved non-Markovian accelerated degradation model is constructed, in which the long-range dependence and unit-to-unit variability are considered and quantified properly.
- A novel statistical inference method to estimate unknown parameters in ADT models is presented based on expectation maximization (EM) algorithm, in which the maximization of the overall likelihood function is achieved.

The organization of the paper is as follows. Firstly, Section 2 gives the preliminary about the FBM. Then, in Section 3, an improved non-Markovian accelerated degradation model is proposed, and a

statistical inference method based on the EM algorithm is developed. After that, the practicability and the superiority of the proposed methodology are verified by a simulation case and an engineering case in Section 4 and Section 5, respectively. Finally, Section 6 concludes the work.

2 Preliminary to fractional Brownian motion

According to [24], a standard FBM can be defined as

$$B_H(t) = \frac{1}{\Gamma\left(H + \frac{1}{2}\right)} \int_{-\infty}^t W_H(t-s) dB(s), \quad (1)$$

where,

$$W_H(t-s) = \begin{cases} (t-s)^{H-1/2}, & 0 \leq s \leq t \\ (t-s)^{H-1/2} - (-s)^{H-1/2}, & s < 0; \end{cases} \quad (2)$$

$\Gamma(\cdot)$ is a gamma function formulated by

$$\Gamma(x) = \int_0^{\infty} t^{x-1} e^{-t} dt; \quad (3)$$

$B(\cdot)$ represents the standard Brownian motion; t is a given time; and H is the Hurst exponent with the range of $(0, 1)$. For the standard FBM shown in (1), the autocorrelation function can be expressed by

$$E[B_H(t)B_H(s)] = \frac{1}{2} \left(t^{2H} + s^{2H} - |t-s|^{2H} \right). \quad (4)$$

It can be seen from equation (4) that the memory effect is determined by H . Depending on the value of H , there are three different cases [17]:

- 1) When $0 < H < 0.5$, the increments of FBM are negatively correlated, which implies that future increments tend to an opposite tendency of the previous direction.
- 2) When $H = 0.5$, the FBM degenerates into the BM, and there is no dependence in the process.
- 3) When $0.5 < H < 1$, the increments of FBM are positively correlated, which implies that future increments tend to follow the previous direction.

We can see that the standard BM is a special case of the standard FBM. In addition, for $t \geq 0$, the standard FBM satisfies the following properties:

- 1) $B_H(0) = 0$;
- 2) $B_H(t) - B_H(s) \sim B_H(t-s)$ for any $s < t$;
- 3) $E[B_H(t)] = 0$ and $E[B_H^2(t)] = t^{2H}$;
- 4) $B_H(at) \sim a^H B_H(t)$ for $a > 0$;

3 Methodology

3.1 Model construction

As mentioned previously, the Markovian ADT models, which assume that current degradation is independent of historical degradation, fail to describe the degradation process with the memory effect.

Moreover, none of the existing ADT models can deal with the coexistence of non-Markovian degradation with long-range dependence and unit-to-unit variability. In this section, we construct an improved non-Markovian accelerated degradation model, in which the degradation process with long-range dependence is described by the FBM and the unit-to-unit variability is analyzed and quantified properly.

3.1.1 Non-Markovian Accelerated Degradation Model based on FBM

In order to describe the non-Markovian degradation process with long-range dependence, FBM is introduced to construct the accelerated degradation model as follows:

$$X(s, t) = f(s, t) + \sigma B_H(t), \quad (5)$$

where $X(\cdot)$ denotes the performance degradation; $f(\cdot)$ is a function of stress s and time t , which depicts the deterministic degradation trend of the product; σ represents the diffusion coefficient. Without loss of generality, the initial degradation is assumed to be zero. If not, $X(s, t) = X(s, t) - X(s, 0)$ will be used [25].

In essence, performance degradation is a substance or energy change process within the product [26]. According to the transport process in statistical physics [27], the change amount in substance or energy can be expressed as the change rate influenced by stresses multiplied by a monotonically increasing function of time. Accordingly, $f(\cdot)$ in (5) can be decoupled as the performance degradation rate function $e(s)$ multiplied by the time scale function $\tau(t)$, i.e.:

$$X(s, t) = e(s) \cdot \tau(t) + \sigma B_H(t), \quad (6)$$

where $\tau(t) = t^\beta$, $\beta > 0$ is a common assumption for the time-scale transformation function [25]. If $\beta = 1$, then it represents a linear degradation process, otherwise a nonlinear degradation process; $e(s)$ is also known as the acceleration model which indicates the relationship between degradation rate and stress [28]. In general, $e(s)$ is usually assumed as a log-linear function as follows:

$$e(s) = \exp(\alpha_0 + \alpha_1 s^*) \quad (7)$$

where $\alpha_0 > 0$ and $\alpha_1 > 0$ are constant unknown parameters; s^* is the standardized stress. For different acceleration models, s^* can be calculated as [29]

$$s^* = \begin{cases} \frac{1/s_0 - 1/s}{1/s_0 - 1/s_H}, & \text{Arrhenius model,} \\ \frac{\ln s - \ln s_0}{\ln s_H - \ln s_0}, & \text{Power law model,} \\ \frac{s - s_0}{s_H - s_0}, & \text{Exponential model,} \end{cases} \quad (8)$$

where s_0 and s_H are the normal and the highest applied stress levels, respectively. The choice of acceleration models mainly depends on the type of accelerated stress. For instance, if the accelerated stress is temperature, the Arrhenius model is adopted; if the accelerated stress is humidity, the Power law model is adopted [30].

3.1.2 Unit-to-unit Variability in Non-Markovian Accelerated Degradation Model

As aforementioned, the unit-to-unit variability plays a significant role in ADT modeling. To be

specific, for a certain product, due to manufacturing imperfections, each item may have its own performance degradation rate [31]. As a result, Since $\tau(t)$ is usually identical for all tested items in a certain stress level, it is reasonable to deduce that each item has unique $e(s)$ in (6). Without other prior information, we assume that the degradation rate of different items follows a normal probability distribution, i.e., $e(s) \sim N(\mu_e(s), \sigma_e^2(s))$, $\mu_e(s) > 0$, $\sigma_e(s) > 0$. Thus, (6) is transformed as

$$X(s, t) = e(s) \cdot \tau(t) + \sigma B_H(t), e(s) \sim N(\mu_e(s), \sigma_e^2(s)). \quad (9)$$

Considering that $e(s)$ is a random variable, the degradation rate function in (6) can be rewritten as

$$e(s) = \exp(\alpha_0 + \alpha_1 s^*) = a \exp(\alpha_1 s^*), \quad (10)$$

where $a = \exp(\alpha_0)$ is a random variable with a normal probability distribution, i.e., $a \sim N(\mu_a, \sigma_a^2)$, $\mu_a > 0$, $\sigma_a > 0$. Then, the distribution parameter $\mu_e(s)$ and $\sigma_e(s)$ can be expressed as

$$\mu_e(s) = \mu_a \exp(\alpha_1 s^*), \sigma_e(s) = \sigma_a \exp(\alpha_1 s^*). \quad (11)$$

3.1.3 Relationship of the proposed model to other ADT models

The non-Markovian ADT model proposed in this paper is described by (8), (9), and (11), which is denoted as M_0 in the following sections. It should be noted that the proposed ADT model has three special cases as follows:

- 1) When the unit-to-unit variability is not considered, i.e., a is a constant, it degenerates into the model in [20], which is denoted as M_1 in the following sections.
- 2) When the non-Markovian degradation is not considered, i.e., $H = 0.5$, it degenerates into the model in [32], which is denoted as M_2 in the following sections.
- 3) When the unit-to-unit variability and the non-Markovian degradation are both not considered, i.e., a is a constant and $H = 0.5$, it degenerates into the model in [33], which is denoted as M_3 in the following sections.

3.2 Lifetime distribution and reliability analysis

The main purpose of ADT is to extrapolate the lifetime distribution and reliability of the product at normal stress s_0 by using the degradation data at high stress levels. A product is considered to fail when its performance degradation accumulates to a critical threshold. Let ω be the critical threshold of the degradation process, then the failure time T of a product can be defined as the first passage time when its degradation exceeds the pre-determined critical threshold value ω , that is

$$T = \inf \{t \mid X(s_0, t) < \omega\}. \quad (12)$$

The reliability of a product is expressed as the probability that a component or system can perform the required function at a given time t under specified operating conditions, which can be expressed as

$$R(t) = \Pr \{T \geq t\}. \quad (13)$$

Due to the complexity of the model, it is difficult to derive an explicit expression for (12) and (13). To solve this problem, we employ the Monte Carlo (MC) method to calculate the lifetime distribution

and reliability of a product at normal stress s_0 . The detailed steps of the MC method are summarized in Algorithm 1. Specifically, to generate a standard FBM path, a fast Fourier transform (FFT) algorithm is utilized [34]. Detailed steps of the FFT algorithm can be found in [20].

<p>Algorithm 1: The MC method to compute the product lifetime distribution and reliability at normal stress s_0</p>
<p>Step 1. Obtain the model parameters $\hat{\theta}$, where $\theta = [\mu_a, \sigma_a^2, \alpha_1, \beta, \sigma^2, H]^T$ (using the maximum likelihood estimation (MLE) approach based on the EM algorithm developed in the subsequent Section 3.3);</p> <p>Step 2. Based on $\hat{\theta}$, simulate N degradation paths at normal stress s_0:</p> <p>For q in $1:N$ (N is the number of MC iterations and should be sufficiently large),</p> <p>2.1 Simulate the q^{th} standard FBM path $B_{H=\hat{H}}^q(t)$ using the FFT algorithm;</p> <p>2.2 Generate a unit-specific a^q according to its distribution $N(\hat{\mu}_a, \hat{\sigma}_a^2)$;</p> <p>2.3 Obtain the degradation path as $X_q(s_0, t) = a^q \exp(\hat{\alpha}_1 s_0^*) \cdot t^{\hat{\beta}} + \hat{\sigma} B_{H=\hat{H}}^q(t)$.</p> <p>Step 3. Compute the product lifetime distribution and reliability at normal stress s_0:</p> <p>3.1 Compute the failure time based on the N simulated degradation paths using (12), denoted as $T_q (1 \leq q \leq N)$;</p> <p>3.2 Obtain an empirical estimate of the product lifetime distribution at stress s_0 as</p> $F(t \hat{\theta}, s_0) = \frac{1}{N} \sum_{q=1}^N 1_t(T_q); 1_t(T_q) = \begin{cases} 1, & \text{if } T_q \leq t \\ 0, & \text{otherwise} \end{cases};$ <p>3.3 Calculate the product reliability at the specific time t using (13).</p>

3.3 Parameter estimation Statistical inference

Based on (9) and (11), the unknown parameters $\theta = [\mu_a, \sigma_a^2, \alpha_1, \beta, \sigma^2, H]^T$ in M_0 need to be determined. In general, θ will be estimated by the observed ADT data in laboratory. In this section, a statistical inference method based on the EM algorithm is developed to estimate the unknown parameters by the constant-stress ADT data.

The observed ADT data x_{lij} is denoted as the j^{th} degradation value of unit i under the l^{th} stress level and t_{lij} is the corresponding measurement time, $l = 1, 2, \dots, k; i = 1, 2, \dots, n_l; j = 1, 2, \dots, m_{li}$, where k is the number of stress levels, n_l is the number of test items under the l^{th} stress level, and m_{li} is the number of measurements for unit i under the l^{th} stress level. Hereby, the degradation observations of the i^{th} item tested at l^{th} stress level can be denoted as $\mathbf{x}_{li} = [x_{li1}, x_{li2}, \dots, x_{li m_{li}}]^T$. Furthermore, we define

$$\boldsymbol{\tau}_{li} = [\tau(t_{li1}), \tau(t_{li2}), \dots, \tau(t_{li m_{li}})]^T \text{ and } \mathbf{B}_{li}^H = [B_H(t_{li1}), B_H(t_{li2}), \dots, B_H(t_{li m_{li}})]^T.$$

Since each product has a unique degradation rate, for the i^{th} item tested at l^{th} stress level, we have

$$\mathbf{x}_{li} = a_{li}\boldsymbol{\psi}_{li} + \sigma\mathbf{B}_H^{li}, \quad (14)$$

where

$$\boldsymbol{\psi}_{li} = \exp(\alpha_1 s_l^*) \boldsymbol{\tau}_{li}. \quad (15)$$

According to the properties of FBM, \mathbf{x}_{li} follows a multivariate normal probability distribution given by

$$\mathbf{x}_{li} \sim N(\mu_a \boldsymbol{\psi}_{li}, \boldsymbol{\Xi}_{li}), \quad (16)$$

where $\boldsymbol{\Xi}_{li}$ is a $K_{li} \times K_{li}$ dimensional covariance matrix and its $(u, v)^{\text{th}}$ entry can be calculated by

$$(\boldsymbol{\Xi}_{li})_{uv} = \sigma_e^2 \tau(t_{liu}) \tau(t_{liv}) + \frac{\sigma^2}{2} (t_{liu}^{2H} + t_{liv}^{2H} - |t_{liu} - t_{liv}|^{2H}). \quad (17)$$

Hence, the likelihood function given \mathbf{x}_{li} can be derived as

$$L_{ij}(\boldsymbol{\theta} | \mathbf{x}_{li}) = (2\pi)^{-\frac{K_{ij}}{2}} |\boldsymbol{\Xi}_{li}|^{-\frac{1}{2}} \exp\left[-\frac{1}{2} (\mathbf{x}_{li} - \mu_a \boldsymbol{\psi}_{li})^T \boldsymbol{\Xi}_{li}^{-1} (\mathbf{x}_{li} - \mu_a \boldsymbol{\psi}_{li})\right]. \quad (18)$$

Next, based on (18), the log-likelihood function given all the observations \mathbf{x} can be expressed as

$$\ln L(\boldsymbol{\theta} | \mathbf{x}) = \sum_{l=1}^k \sum_{i=1}^{n_l} \ln L_{ij}(\boldsymbol{\theta} | \mathbf{x}_{li}). \quad (19)$$

In order to obtain the estimate of $\boldsymbol{\theta}$, we need to maximize the log-likelihood function (19). However, the unobservability of a_{li} makes the direct constrained optimization of the log-likelihood function very tough, and generally hard to get converge to a solution. Therefore, a two-step MLE method was proposed and to estimate the unknown parameters in ADT models considering unit-to-unit variability [25, 32]. Nevertheless, the two-step MLE method obtains local maximization of two likelihood functions rather than maximizing the overall likelihood function. This will deviate the parameter estimations from the actual data, thus affecting the precision of reliability and lifetime assessments, especially when the degradation process has a complex property like long-range dependence.

To address this issue, we propose a parameter estimation method based on the EM algorithm [35]. The main idea of the EM algorithm lies in substituting the unobservable variables with their conditional expectations, where the parameter updates at each step can be obtained in a closed form or a simple form [36]. The EM algorithm consists of two steps: the expectation-step (E-step) and the maximization step (M-step). During the E-step, the expectation of the log-likelihood is computed with respect to the latent variables, and the M-step determines the maximizer of this expected likelihood. The two steps are repeated iteratively until satisfactory convergence is achieved.

We denote $\boldsymbol{\Omega} = \{a_{11}, \dots, a_{1n_1}, a_{21}, \dots, a_{ln_l}\}$, then given the complete data including \mathbf{x} and $\boldsymbol{\Omega}$, the complete log-likelihood function can be written as

$$\ln L(\boldsymbol{\theta} | \mathbf{x}, \boldsymbol{\Omega}) = \sum_{l=1}^k \sum_{i=1}^{n_l} \left[\ln p(\mathbf{x}_{li} | a_{li}, \boldsymbol{\theta}) + \ln p(a_{li} | \boldsymbol{\theta}) \right], \quad (20)$$

where $p(\mathbf{x}_{li} | a_{li}, \boldsymbol{\theta})$ denotes the probability density function (PDF) of \mathbf{x}_{li} given a_{li} and $\boldsymbol{\theta}$; and $p(a_{li} | \boldsymbol{\theta})$ denotes the PDF of a_{li} given $\boldsymbol{\theta}$. According to the ADT models (9) and (11), (20) can be extended as

$$\begin{aligned} \ln L(\boldsymbol{\theta}|\mathbf{x}, \boldsymbol{\Omega}) = & -\frac{1}{2} \sum_{l=1}^k \sum_{i=1}^{n_l} \left\{ m_{li} \ln(2\pi) + \ln |\mathbf{Q}_{li}| + (\mathbf{x}_{li} - a_{li} \boldsymbol{\psi}_{li})^T \mathbf{Q}_{li}^{-1} (\mathbf{x}_{li} - a_{li} \boldsymbol{\psi}_{li}) \right\} \\ & - \frac{1}{2} \sum_{l=1}^k \sum_{i=1}^{n_l} \left\{ \ln(2\pi) + \ln \sigma_a^2 + \frac{(a_{li} - \mu_a)^2}{\sigma_a^2} \right\} \end{aligned} \quad (21)$$

where \mathbf{Q}_{li} is a $K_{li} \times K_{li}$ dimensional covariance matrix and its $(u, v)^{\text{th}}$ entry can be calculated by

$$\left(\mathbf{Q}_{li} \right)_{uv} = \frac{\sigma^2}{2} \left(t_{liu}^{2H} + t_{liv}^{2H} - |t_{liu} - t_{liv}|^{2H} \right). \quad (22)$$

To facilitate the following statistical inference, the unknown parameters are re-parameterized by

$\boldsymbol{\Sigma}_{li} = \frac{\mathbf{Q}_{li}}{\sigma^2}$. Then, (21) can be rewritten as

$$\begin{aligned} \ln L(\boldsymbol{\theta}|\mathbf{x}, \boldsymbol{\Omega}) = & -\frac{1}{2} \sum_{l=1}^k \sum_{i=1}^{n_l} (m_{li} + 1) \ln(2\pi) - \frac{1}{2} \sum_{l=1}^k \frac{n_l}{2} \ln \sigma_a^2 - \frac{1}{2} \sum_{l=1}^k \sum_{i=1}^{n_l} \frac{m_{li} n_l}{2} \ln \sigma^2 \\ & - \frac{1}{2} \sum_{l=1}^k \sum_{i=1}^{n_l} \ln |\boldsymbol{\Sigma}_{ij}| - \frac{1}{2} \sum_{l=1}^k \sum_{i=1}^{n_l} \left[\frac{(\mathbf{x}_{li} - a_{li} \boldsymbol{\psi}_{li})^T \boldsymbol{\Sigma}_{li}^{-1} (\mathbf{x}_{li} - a_{li} \boldsymbol{\psi}_{li})}{\sigma^2} + \frac{(a_{li} - \mu_a)^2}{\sigma_a^2} \right] \end{aligned} \quad (23)$$

Considering the update of $\boldsymbol{\theta}$ during the iterations in the EM algorithm, let $\boldsymbol{\theta}^{(p)} = \left[\mu_a^{(p)}, \sigma_a^{2(p)}, \alpha_1^{(p)}, \beta^{(p)}, \sigma^{2(p)}, H^{(p)} \right]^T$ represent the estimations in the p^{th} step. To calculate the expectation of the log-likelihood function (23), we need to obtain the first and second moments of a_{li} conditional on \mathbf{x}_{li} and $\boldsymbol{\theta}^{(p)}$. It is easily found that the posterior distribution of a_{li} conditional on \mathbf{x}_{li} and $\boldsymbol{\theta}^{(p)}$ is still normally distributed [37]. In the Bayesian framework, the posterior distribution of a_{li} can be obtained as follows

$$\begin{aligned} p(a_{li} | \mathbf{x}_{li}, \boldsymbol{\theta}^{(p)}) & \propto p(\mathbf{x}_{li} | a_{li}, \boldsymbol{\theta}^{(p)}) p(a_{li} | \boldsymbol{\theta}^{(p)}) \\ & \propto \exp \left[-\frac{1}{2} \frac{(\mathbf{x}_{li} - a_{li} \boldsymbol{\psi}_{li}^{(p)})^T \left[\boldsymbol{\Sigma}_{li}^{(p)} \right]^{-1} (\mathbf{x}_{li} - a_{li} \boldsymbol{\psi}_{li}^{(p)})}{\sigma^{2(p)}} \right] \exp \left[-\frac{(a_{li} - \mu_a^{(p)})^2}{2\sigma_a^{2(p)}} \right] \\ & \propto \exp \left\{ -\frac{1}{2} \left[\left(\frac{\left[\boldsymbol{\psi}_{li}^{(p)} \right]^T \left[\boldsymbol{\Sigma}_{li}^{(p)} \right]^{-1} \boldsymbol{\psi}_{li}^{(p)}}{\sigma^{2(p)}} + \frac{1}{\sigma_a^{2(p)}} \right) a_{li}^2 - 2 \left(\frac{\mathbf{x}_{li}^T \left[\boldsymbol{\Sigma}_{li}^{(p)} \right]^{-1} \boldsymbol{\psi}_{li}^{(p)}}{\sigma^{2(p)}} + \frac{\mu_a^{(p)}}{\sigma_a^{2(p)}} \right) a_{li} \right] \right\} \\ & \propto \exp \left[-\frac{\left[a_{li} - \left(\mathbf{x}_{li}^T \left[\boldsymbol{\Sigma}_{li}^{(p)} \right]^{-1} \boldsymbol{\psi}_{li}^{(p)} \sigma_a^{2(p)} + \mu_a^{(p)} \sigma^{2(p)} \right) / \left(\left[\boldsymbol{\psi}_{li}^{(p)} \right]^T \left[\boldsymbol{\Sigma}_{li}^{(p)} \right]^{-1} \boldsymbol{\psi}_{li}^{(p)} \sigma_a^{2(p)} + \sigma^{2(p)} \right) \right]^2}{2\sigma^{2(p)} \sigma_a^{2(p)} / \left(\left[\boldsymbol{\psi}_{li}^{(p)} \right]^T \left[\boldsymbol{\Sigma}_{li}^{(p)} \right]^{-1} \boldsymbol{\psi}_{li}^{(p)} \sigma_a^{2(p)} + \sigma^{2(p)} \right)} \right] \\ & \sim N \left(\mu_{li}^{(p)}, \sigma_{li}^{2(p)} \right) \end{aligned} \quad (24)$$

with

$$\mu_{li}^{(p)} = \frac{\mathbf{x}_{li}^T \left[\boldsymbol{\Sigma}_{li}^{(p)} \right]^{-1} \boldsymbol{\psi}_{li}^{(p)} \sigma_a^{2(p)} + \mu_a^{(p)} \sigma^{2(p)}}{\left[\boldsymbol{\psi}_{li}^{(p)} \right]^T \left[\boldsymbol{\Sigma}_{li}^{(p)} \right]^{-1} \boldsymbol{\psi}_{li}^{(p)} \sigma_a^{2(p)} + \sigma^{2(p)}}, \quad (25)$$

$$\sigma_{li}^{2(p)} = \frac{\sigma^{2(p)} \sigma_a^{2(p)}}{\left[\boldsymbol{\psi}_{li}^{(p)} \right]^T \left[\boldsymbol{\Sigma}_{li}^{(p)} \right]^{-1} \boldsymbol{\psi}_{li}^{(p)} \sigma_a^{2(p)} + \sigma^{2(p)}}. \quad (26)$$

In the following, we use the EM algorithm to estimate $\boldsymbol{\theta}$ iteratively. To be specific, the E-step computes the expectation $Q(\boldsymbol{\theta} | \mathbf{x}, \boldsymbol{\theta}^{(p)})$ of $\ln L(\boldsymbol{\theta} | \mathbf{x}, \boldsymbol{\Omega})$ with respect to $\boldsymbol{\Omega}$. According to (23), (25) and (26), we have

$$\begin{aligned} Q(\boldsymbol{\theta} | \mathbf{x}, \boldsymbol{\theta}^{(p)}) &= E_{\boldsymbol{\Omega} | \boldsymbol{\theta}^{(p)}}[\ln L(\boldsymbol{\theta} | \mathbf{x}, \boldsymbol{\Omega})] \\ &= -\frac{1}{2} \sum_{l=1}^k \sum_{i=1}^{n_l} (m_{li} + 1) \ln(2\pi) - \frac{1}{2} \sum_{l=1}^k \frac{n_l}{2} \ln \sigma_a^2 - \frac{1}{2} \sum_{l=1}^k \sum_{i=1}^{n_l} \frac{m_{li} n_l}{2} \ln \sigma^2 \\ &\quad - \frac{1}{2} \sum_{l=1}^k \sum_{i=1}^{n_l} \ln |\boldsymbol{\Sigma}_{li}| - \frac{1}{2} \sum_{l=1}^k \sum_{i=1}^{n_l} \frac{\left[\mu_{li}^{(p)} \right]^2 + \sigma_{li}^{2(p)} - 2\mu_{li}^{(p)} \mu_a + \mu_a^2}{\sigma_a^2} \\ &\quad - \frac{1}{2} \sum_{l=1}^k \sum_{i=1}^{n_l} \frac{\mathbf{x}_{li}^T \boldsymbol{\Sigma}_{li}^{-1} \mathbf{x}_{li} - 2\mu_{li}^{(p)} \mathbf{x}_{li}^T \boldsymbol{\Sigma}_{li}^{-1} \boldsymbol{\psi}_{li} + \left(\left[\mu_{li}^{(p)} \right]^2 + \sigma_{li}^{2(p)} \right) \boldsymbol{\psi}_{li}^T \boldsymbol{\Sigma}_{li}^{-1} \boldsymbol{\psi}_{li}}{\sigma^2} \end{aligned} \quad (27)$$

In the M-step, by taking the first partial derivatives of $Q(\boldsymbol{\theta} | \mathbf{x}, \boldsymbol{\theta}^{(p)})$ with regard to μ_a , σ_a^2 and σ^2 , respectively, and setting each derivative to be zero, we have

$$\mu_a^{(p+1)} = \frac{\sum_{l=1}^k \sum_{i=1}^{n_l} \mu_{li}^{(p)}}{\sum_{l=1}^k n_l} \quad (28)$$

$$\sigma_a^{2(p+1)} = \frac{\sum_{l=1}^k \sum_{i=1}^{n_l} \left(\left[\mu_{li}^{(p)} \right]^2 + \sigma_{li}^{2(p)} - 2\mu_{li}^{(p)} \mu_a^{(p+1)} + \left[\mu_a^{(p+1)} \right]^2 \right)}{\sum_{l=1}^k n_l} \quad (29)$$

$$\sigma^{2(p+1)} = \frac{\sum_{l=1}^k \sum_{i=1}^{n_l} \left(\mathbf{x}_{li}^T \boldsymbol{\Sigma}_{li}^{-1} \mathbf{x}_{li} - 2\mu_{li}^{(p)} \mathbf{x}_{li}^T \boldsymbol{\Sigma}_{li}^{-1} \boldsymbol{\psi}_{li} + \left(\left[\mu_{li}^{(p)} \right]^2 + \sigma_{li}^{2(p)} \right) \boldsymbol{\psi}_{li}^T \boldsymbol{\Sigma}_{li}^{-1} \boldsymbol{\psi}_{li} \right)}{\sum_{l=1}^k \sum_{i=1}^{n_l} m_{li}}. \quad (30)$$

Note that $\sigma^{2(p+1)}$ depends on the estimates of α_1 , β and H . Hence, by substituting $\mu_a^{(p+1)}$, $\sigma_a^{2(p+1)}$ and $\sigma^{2(p+1)}$ into (27), the estimates of $\alpha_1^{(p+1)}$, $\beta^{(p+1)}$ and $H^{(p+1)}$ can be achieved by maximizing the profile likelihood function through a three-dimensional search. Next, by substituting $\alpha_1^{(p+1)}$, $\beta^{(p+1)}$ and $H^{(p+1)}$ into (30), we can obtain the estimate of $\sigma^{2(p+1)}$. The iterations are often terminated when the

relative change of the parameter estimations falls below a predefined threshold ε , or when the number of iterations reaches a fixed threshold. The complete algorithm is summarized as shown in Algorithm 2.

Algorithm 2: Parameter Estimations Using the EM Algorithm	
Step 1. Initialize $\theta^{(0)} = [\mu_a^{(0)}, \sigma_a^{(0)}, \alpha_1^{(0)}, \beta^{(0)}, \sigma^{(0)}, H^{(0)}]^T$ and ε . Set $p = 0$.	
Step 2. Get $\theta^{(p+1)}$ by using the EM algorithm	
E-step:	
2.1 Calculate $\mu_{ii}^{(p)}$ and $\sigma_{ii}^{2(p)}$ by using (25) and (26);	
M-step:	
2.2 Update $\mu_a^{(p+1)}$ and $\sigma_a^{2(p+1)}$ by using (28) and (29);	
2.3 Update $\alpha_1^{(p+1)}$, $\beta^{(p+1)}$ and $H^{(p+1)}$ by substituting $\mu_a^{(p+1)}$, $\sigma_a^{2(p+1)}$ and (30) into (27) and maximizing the profile likelihood function through a three-dimensional search;	
2.4 Update $\sigma^{2(p+1)}$ by substituting $\alpha_1^{(p+1)}$, $\beta^{(p+1)}$ and $H^{(p+1)}$ into (30).	
Step 3. If $ \theta^{(p+1)} - \theta^{(p)} \leq \varepsilon$, obtain $\hat{\theta} = [\mu_a^{(p+1)}, \sigma_a^{2(p+1)}, \alpha_1^{(p+1)}, \beta^{(p+1)}, \sigma^{2(p+1)}, H^{(p+1)}]^T$. Otherwise, go to Step 2.	

4 Simulation study

In this section, the proposed method is illustrated through a numerical simulation case. Furthermore, we demonstrate the superiority of the proposed parameter estimation method and the significance of the proposed ADT model.

4.1 Simulation settings

Detailed information on the constant-stress ADT simulation case is shown in Table 1. The degradation exhibits negatively correlated long-range dependence because $H = 0.1$. Specifically, the sample sizes for each stress level (N) are set as 6 and the measurements for each sample (M) are set as 10.

Table 1 Information for simulation settings.

Content	Values
Accelerated stress level (Temperature/ $^{\circ}$ C)	80, 100, 120
Normal stress level ($^{\circ}$ C)	40
Degradation model	$X(s, t) = a \exp(\alpha_1 s^*) \cdot t^\beta + \sigma B_H(t)$, $a \sim N(\mu_a, \sigma_a^2)$.
Acceleration model	Arrhenius model
Parameter value: $\mu_a, \sigma_a, \alpha_1, \beta, \sigma, H$	1e-5, 2e-6, 2.5, 1.5, 0.1, 0.1
Inspection interval (h)	100

4.2 Results and analysis

In this case, the initial value of θ is taken from the estimations of the two-step MLE method. The terminated threshold ε for the EM algorithm iteration is set as 0.01. Subsequently, according to Algorithm 2, we obtain the estimations of unknown parameters as shown in Table 2. From Table 2, it can be seen that the estimations are basically close to the true values.

Table 2 Estimated results of θ in the simulation case.

Parameters	μ_a	σ_a	α_1	β	σ	H
Values	9.144e-6	9.559e-7	2.286	1.534	0.104	0.073

For further exhibiting the effectiveness of the proposed methodology, the predicted deterministic degradation trends, upper and lower boundaries of 10000 simulated degradation paths at 90% confidence level and actual observations under 80°C, 100°C and 120°C are plotted in Fig. 1. As can be seen in Fig. 1, under all accelerated stress levels, the predicted deterministic degradation trends primarily lie in the observations, and the boundaries nicely envelope the observations.

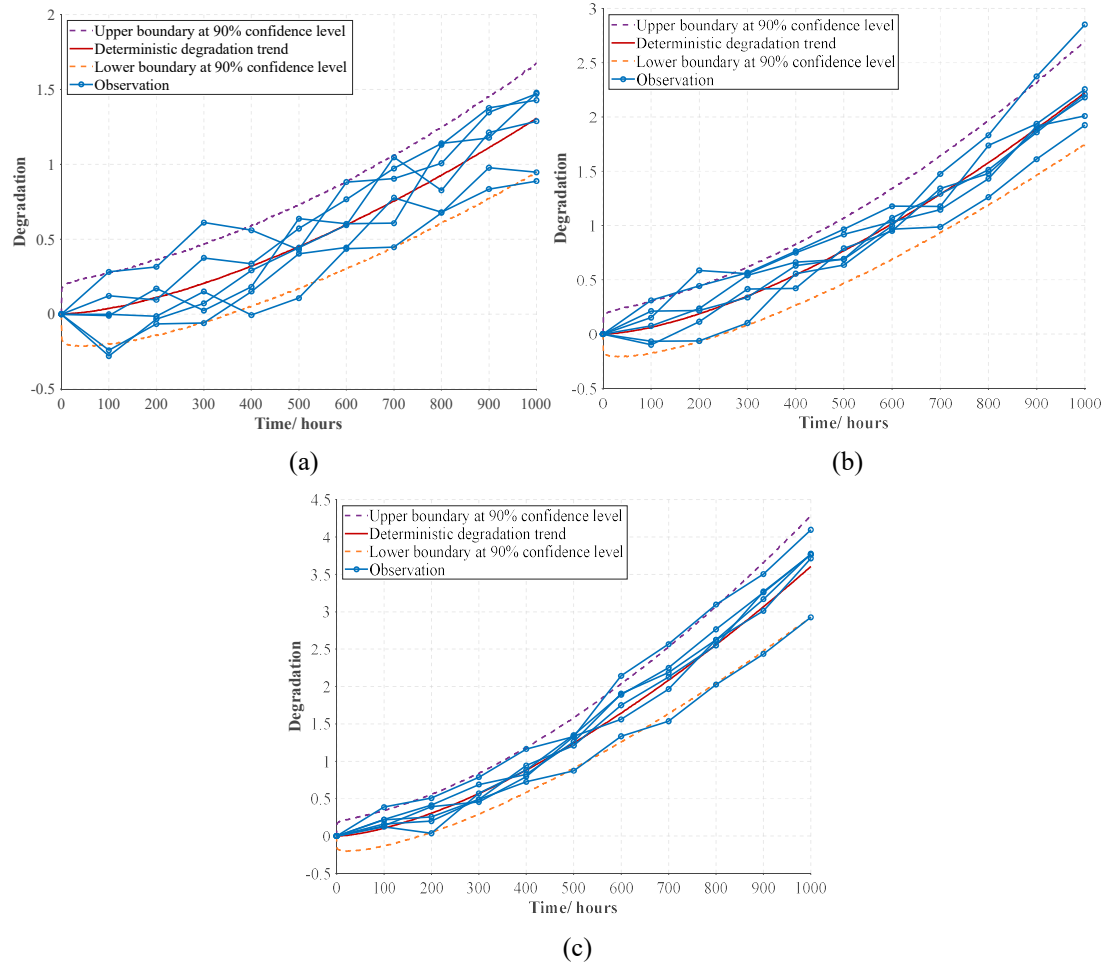


Fig. 1 Deterministic degradation trend, boundaries and observations: (a) 80°C (b) 100°C (c) 120°C.

Next, the predicted deterministic degradation trend with time and temperature is shown in Fig. 2, which describes the degradation accumulation at a given time and temperature. It can be seen that degradation increases with the increase of time and temperature.

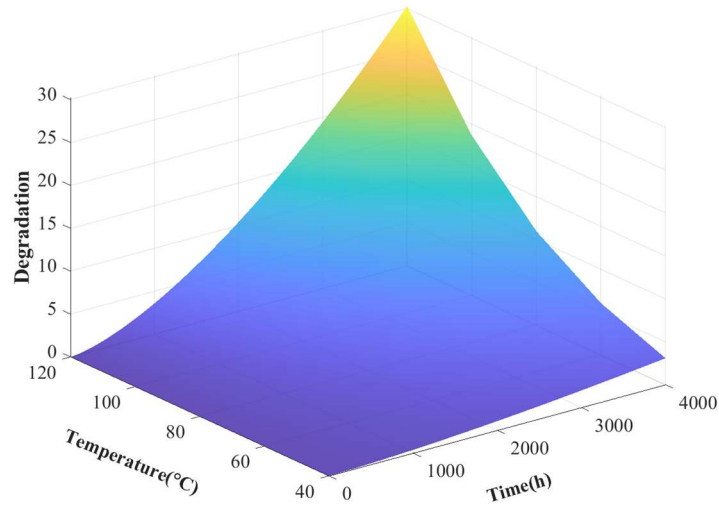


Fig. 2 Deterministic degradation trend with time and temperature.

Finally, according to Algorithm 1, when the failure threshold of the product is 5, we can estimate the lifetime distribution and reliability of the product under the normal use condition (40°C) as shown in Fig. 3 and Fig. 4, respectively. From Fig. 4, we can get the reliability of the product for a given operating time. For example, when the product is operated for 4613 hours, its reliability is 0.99. The results can provide guidance for the development of maintenance and warranty strategies.

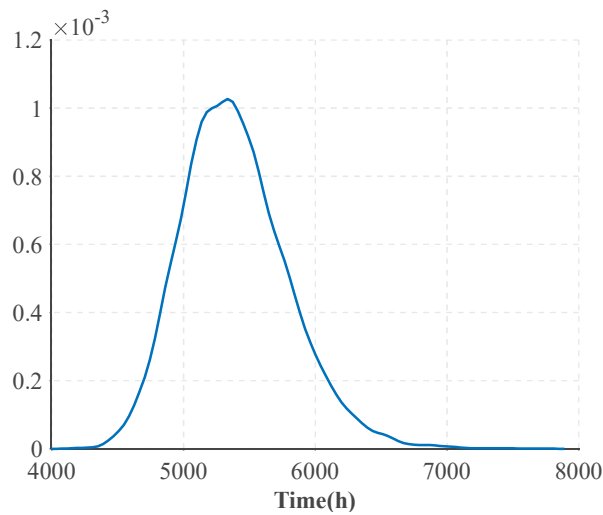


Fig. 3 Lifetime distribution of the product under normal stress level (40°C).

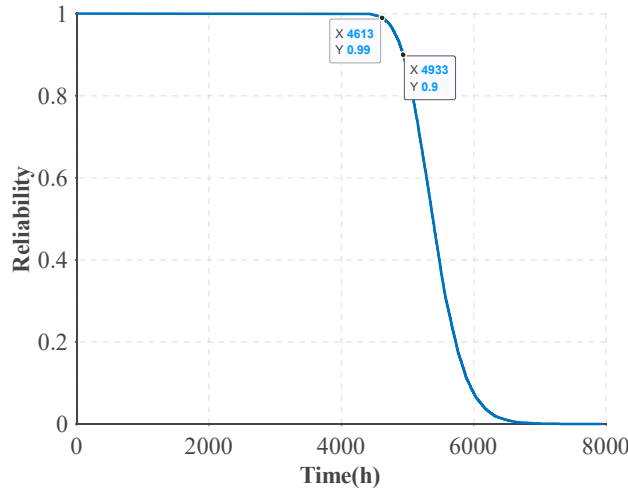


Fig. 4 Reliability of the product under normal stress level (40°C).

4.3 Discussions

4.3.1 Comparison of parameter estimation methods

In order to illustrate the superiority of the proposed parameter estimation method compared to the existing two-step MLE method [25, 32], in this subsection, nine combinations of (N, M) are chosen to generate simulated ADT data. Other simulation settings are the same as in Table 1. For each combination, we obtain the parameter estimations by using these two methods. Then, we compare the maximum value of the log-likelihood function l_{\max} and the relative errors (RE) between the estimations and the true values, so as to achieve a quantitative comparison. The RE of the parameter estimation is computed by

$$RE = \frac{\text{Estimated.value} - \text{True.value}}{\text{True.value}}. \quad (31)$$

Obviously, the closer RE is to 0, the higher the accuracy of the parameter estimations.

Table 3 gives the estimations of unknown parameters for two methods under nine combinations of sample sizes and measurements. Fig. 5 illustrates the RE for two methods under different combinations. From Table 3 and Fig. 5, we can get the following results:

- For the two-step MLE method, when the number of measurements is small, the estimation of H is highly biased. As the number of measurements increases, the estimation of H comes closer to the true value but is still unsatisfactory. On the other hand, for the EM algorithm, when the number of measurements is small, the estimation of H is acceptable. As the number of measurements increases, the estimation of H is very close to the true value. This illustrates the significance of maximizing the overall likelihood function for parameter estimations, especially when degradation has the long-range dependence property and the number of measurements is small.
- As the sample sizes and measurements increase, the RE obtained by these two estimation methods both decreases, indicating that increasing the information from the ADT experiment can improve the accuracy of parameter estimations effectively.
- In all combinations, the l_{\max} and RE obtained by the EM algorithm are better than those of the two-step MLE method, proving the superiority of the proposed estimation method.

Table 3 Parameter estimations for two methods under nine combinations of sample sizes and measurements.

(N,M)	Method	μ_a	σ_a	α_1	β	σ	H	l_{\max}	RE
(6,10)	two-step MLE	9.119e-6	1.154e-6	2.243	1.539	0.145	2.948e-8	103.838	2.089
	EM algorithm	9.144e-6	9.559e-7	2.286	1.534	0.104	0.073	105.613	1.025
(6,20)	two-step MLE	1.142e-5	2.650e-6	2.333	1.505	0.151	0.029	146.232	1.757
	EM algorithm	1.142e-5	2.635e-6	2.329	1.506	0.116	0.082	149.298	0.871
(6,30)	two-step MLE	8.852e-6	1.345e-6	2.481	1.515	0.129	0.047	281.194	1.279
	EM algorithm	8.852e-6	1.340e-6	2.482	1.515	0.109	0.079	283.219	0.762
(12,10)	two-step MLE	1.303e-5	2.702e-6	2.121	1.494	0.156	1.134e-8	167.828	2.376
	EM algorithm	1.302e-5	2.640e-6	2.135	1.492	0.138	0.033	169.207	1.830
(12,20)	two-step MLE	1.320e-5	2.550e-6	2.215	1.492	0.138	0.031	357.171	1.781
	EM algorithm	1.320e-5	2.527e-6	2.214	1.493	0.101	0.091	363.958	0.802
(12,30)	two-step MLE	1.110e-5	1.811e-6	2.470	1.491	0.124	0.059	528.113	0.880
	EM algorithm	1.110e-5	1.802e-6	2.470	1.491	0.103	0.096	532.326	0.297
(18,10)	two-step MLE	1.182e-5	2.915e-6	2.297	1.494	0.164	1.584e-8	218.202	2.364
	EM algorithm	1.185e-5	2.727e-6	2.322	1.490	0.091	0.123	228.288	0.946
(18,20)	two-step MLE	9.275e-6	2.153e-6	2.692	1.493	0.154	0.016	495.731	1.610
	EM algorithm	9.273e-6	2.144e-6	2.689	1.493	0.110	0.081	508.612	0.515
(18,30)	two-step MLE	8.724e-6	2.085e-6	2.581	1.505	0.121	0.062	784.706	0.795
	EM algorithm	8.724e-6	2.080e-6	2.581	1.506	0.101	0.098	790.515	0.234

Note: N is the sample size for each stress level, and M is the number of measurements for each sample.

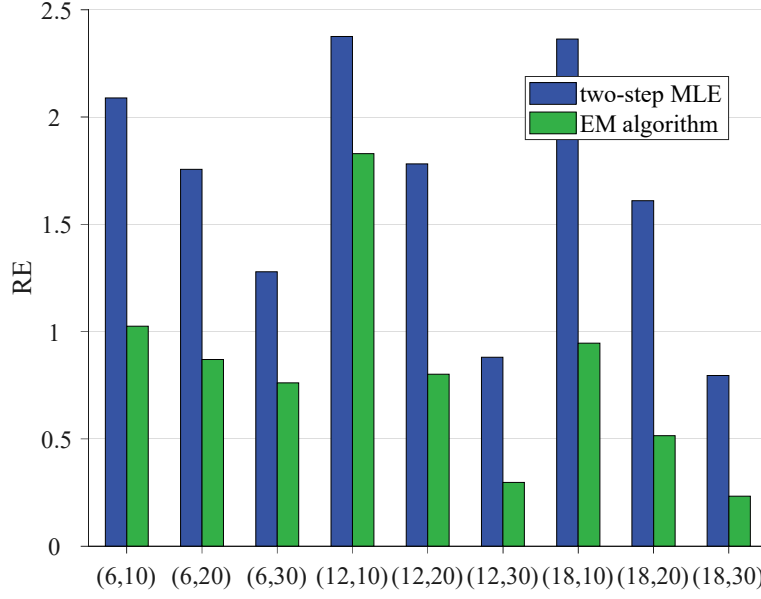


Fig. 5 RE for two methods under nine combinations of sample sizes and measurements.

4.3.2 Comparison of ADT models

In order to illustrate the significance of the proposed ADT model compared to other ADT models mentioned in Section 3.1.3, in this subsection, we set the combination of (N, M) as $(12, 30)$ to generate ADT simulation data. Other simulation settings are the same as in Table 1. For the model M_0 and M_2 , the statistical inference method based on EM algorithm is used for parameter estimations. For the model M_1 and M_3 , the parameters are obtained by directly maximizing the log-likelihood function. Then, we calculate the l_{\max} and the Akaike information criterion (AIC) for each ADT model, so as to achieve a quantitative comparison. The AIC is expressed as [38]

$$AIC = -2l_{\max} + 2n_p, \quad (32)$$

where n_p is the number of unknown parameters. The AIC quantifies how well the model fits the data. The lower the AIC value is, the better the model fits.

Table 4 gives the estimations of unknown parameters for the four ADT models. Clearly, from l_{\max} and AIC values, M_0 is the most suitable model, then is model M_2 , followed by model M_1 , and the worst is model M_3 . The reason is that the model M_2 and M_1 partially consider the unit-to-unit variability and the long-range dependence, respectively. Therefore, they both perform worse than the model M_0 , which considers the unit-to-unit variability and the long-range dependence simultaneously. Moreover, model M_1 even gets wrong degradation law, i.e., the degradation process exhibits positively correlated long-range dependence, which is due to the lack of consideration of the unit-to-unit variability. As for the model M_3 , both the unit-to-unit variability and the long-range dependence are not considered, which leads to the poorest fitting results.

Table 4 Parameter estimations for the four ADT models.

Model	μ_a	σ_a	α_1	β	σ	H	l_{\max}	AIC
M_0	1.110e-5	1.802e-6	2.470	1.491	0.103	0.096	532.326	-1052.65

M_1	9.800e-6	/	2.404	1.513	0.013	0.561	308.210	-606.42
M_2	1.031e-5	1.539e-6	2.521	1.495	0.016	/	392.799	-775.60
M_3	9.063e-6	/	2.670	1.501	0.016	/	266.943	-525.89

In addition, the lifetime distribution and reliability of the product under normal stress level (40°C) for the four ADT models with the real values are illustrated in Fig. 6 and Fig. 7, respectively. It is evident that model M_0 gives the most accurate inference results compared to other ADT models, especially in the high reliability part of concern (i.e., the reliability range from 0.9 to 1), proving the superiority of the proposed ADT model.

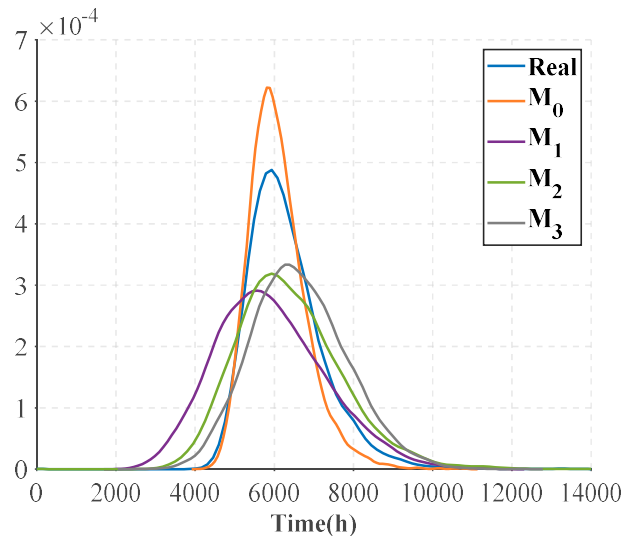


Fig. 6 Lifetime distribution of the product under normal stress level (40°C) for the four ADT models with the real values.

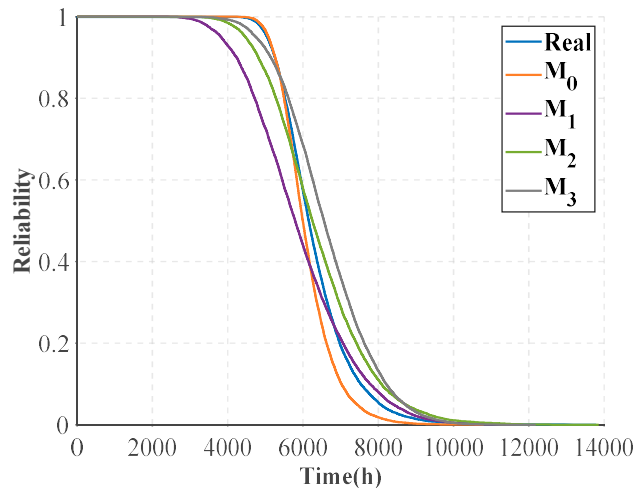


Fig. 7 Reliability of the product under normal stress level (40°C) for the four ADT models with the real values.

5 Engineering application

In this section, we take the accelerated degradation data of microwave electronic assembly to

illustrate our method and compare it with other ADT models.

5.1 Data description

A tuner is a long-lifetime microwave electronic assembly designed primarily for reception, filtering, amplification and gain control of cable signals. Previous investigations into tuner failures have shown the significant impact of temperature on the degradation process [39]. To evaluate the reliability of the tuner, a constant-stress ADT based on temperature was performed under 4 stress levels (55°C, 70°C, 80°C and 85°C). And, the key performance parameter, noise, was measured every ten hours by a computerized measuring system. The number of measurements under each stress level is 50, 35, 31, 23. Fig. 8 illustrates detailed degradation data.

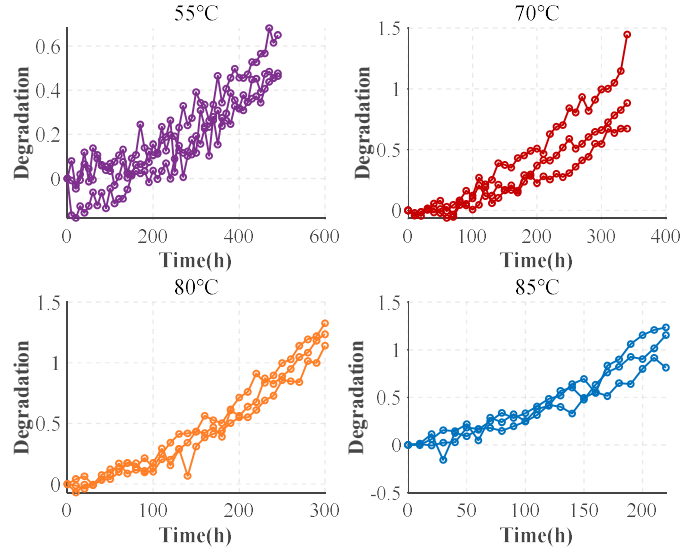


Fig. 8 Accelerated degradation data of microwave electronic assembly under 4 stress levels.

5.2 Modeling and analysis

Since the accelerated stress is temperature, the Arrhenius model is selected to construct the acceleration model. Then, stress normalization is employed according to (8), where the normal stress level is 20°C. Next, based on the two-step MLE method [25, 32], the initial values of the unknown parameters are set as $\theta^{(0)} = [1e-6, 2e-7, 4, 1.5, 0.01, 1e-7]^T$, and the terminated threshold ε for the EM algorithm iteration is set as 0.01. Subsequently, according to Algorithm 2, we obtain the estimations of unknown parameters as shown in Table 5. From Table 5, it can be deduced that the degradation of the electronic assembly exhibits negatively correlated long-range dependence because $H < 0.5$.

Table 5 Estimated results of θ in the microwave case.

Parameters	μ_a	σ_a	α_1	β	σ	H
Values	1.073e-6	1.894e-7	4.667	1.691	0.073	2.497e-8

Then, according to Algorithm 1, when the failure threshold is 7, we can estimate the lifetime distribution and reliability of the electronic assembly under the normal use condition (20°C) as illustrated in Fig. 9 and Fig. 10, respectively. From Fig. 10, we can get some valuable information for the

development of maintenance and warranty strategies: when the electronic assembly is operated for 8639 hours, the reliability of the electronic assembly is 0.99; when the electronic assembly is operated for 9384 hours, the reliability of the product is 0.9.

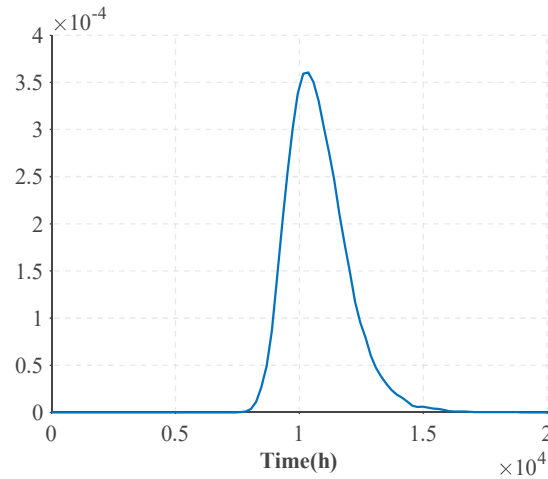


Fig. 9 Lifetime distribution of the electronic assembly under normal stress level (20°C).

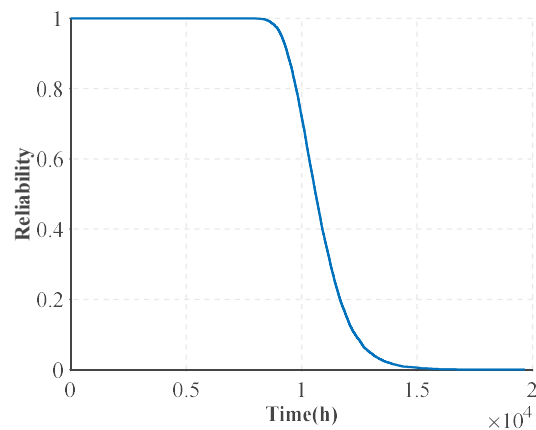


Fig. 10 Reliability of the electronic assembly under normal stress level (20°C).

5.3 Discussions

In general, the better the model fits the degradation data, the greater the potential for the model to reflect the degradation law of the product. Besides, it should be recalled that the ultimate goal of modeling ADT data is to extrapolate the lifetime and reliability of the product under the normal use condition, so it is crucial to ensure the accuracy of the degradation prediction for unseen stress levels. To this end, in the following, we will discuss the fitting and extrapolation capabilities of the proposed model M_0 compared to other ADT models mentioned in Section 3.1.3.

5.3.1 Comparison of model fitting

In this subsection, we first calculate the l_{\max} and the AIC to compare the effectiveness of different ADT models in fitting the degradation data. The parameter estimation methods for the four ADT models are the same as in Section 0. Table 6 gives the estimations of unknown parameters for the four ADT models. As can be seen in Table 6, from l_{\max} and AIC values, M_0 is the most suitable model since it

considers the unit-to-unit variability and the long-range dependence simultaneously.

Table 6 Parameter estimations for the four ADT models in the microwave case.

Model	μ_a	σ_a	α_1	β	σ	H	l_{\max}	AIC
M_0	1.073e-6	1.894e-7	4.667	1.691	0.073	2.497e-8	579.444	-1146.888
M_1	1.349e-6	/	4.518	1.674	0.056	0.1113	551.784	-1093.568
M_2	1.072e-6	2.113e-8	4.473	1.723	0.023	/	479.348	-948.696
M_3	1.601e-6	/	4.280	1.684	0.023	/	479.483	-950.966

Furthermore, in order to quantitatively compare the performance of different ADT models in describing the real degradation data, we set up three comparison indices \overline{ER} , \overline{ER}^U , and \overline{ER}^L to calculate the accuracy of predicted deterministic degradation trend and uncertainty quantification [26]. Specifically, for each ADT model, we generate 1000 degradation paths according to the estimations in Table 6 and calculate the predicted deterministic degradation trend x_{ij}^{pre} , predicted upper boundary x_{ij}^{pre-U} and predicted lower boundary x_{ij}^{pre-L} at t_{ij} under the l^{th} stress level. Then, the three comparison indices can be calculated. The calculations are shown in (33), where $\text{mean}\left\{x_{lij}^{sim}\right\}_{1 \leq i \leq 1000}$, $\text{quantile}\left\{x_{lij}^{sim}\right\}_{5\%}^U$ and $\text{quantile}\left\{x_{lij}^{sim}\right\}_{5\%}^L$ denote the mean value, upper 5% quantile and lower 5% quantile for the 1000 simulated degradation paths, respectively.

$$\begin{aligned}
\overline{ER} &= \frac{1}{k} \sum_{i=1}^k \overline{ER}_i, \overline{ER}_l = \frac{1}{n_l} \sum_{j=1}^{m_i} ER_{ij}, ER_{ij}^L = \frac{|x_{ij}^{pre} - \bar{x}_{lj}|}{\bar{x}_{lj}}, \bar{x}_{lj} = \frac{1}{n_l} \sum_{j=1}^{m_i} x_{lij}, x_{ij}^{pre} = \text{mean}\left\{x_{lij}^{sim}\right\}_{1 \leq i \leq 1000} \\
\overline{ER}^U &= \frac{1}{k} \sum_{i=1}^k \overline{ER}_i^U, \overline{ER}_l^U = \frac{1}{n_l} \sum_{j=1}^{m_i} ER_{ij}^U, ER_{ij}^U = \frac{|x_{ij}^{pre-U} - x_{ij}^U|}{x_{ij}^U}, x_{ij}^U = \max_{1 \leq i \leq n_l} \{x_{lij}\}, x_{ij}^{pre-U} = \text{quantile}\left\{x_{lij}^{sim}\right\}_{5\%}^U \\
\overline{ER}^L &= \frac{1}{k} \sum_{i=1}^k \overline{ER}_i^L, \overline{ER}_l^L = \frac{1}{n_l} \sum_{j=1}^{m_i} ER_{ij}^L, ER_{ij}^L = \frac{|x_{ij}^{pre-L} - x_{ij}^L|}{x_{ij}^L}, x_{ij}^L = \min_{1 \leq i \leq n_l} \{x_{lij}\}, x_{ij}^{pre-L} = \text{quantile}\left\{x_{lij}^{sim}\right\}_{5\%}^L
\end{aligned} \tag{33}$$

It can be seen that the closer \overline{ER}_l is to 0, the more accurately the model predicts the deterministic degradation trend under the l^{th} stress level. The closer \overline{ER}_l^U or \overline{ER}_l^L is to 0, the better the predicted boundary can describe the uncertainty of the real data under the l^{th} stress level. Moreover, \overline{ER} , \overline{ER}^U , and \overline{ER}^L reflect the predicted performance of an ADT model under all stress levels.

Table 7 gives the quantitative indices for the four ADT models under all stress levels. The visualization results of the deterministic degradation trend and the degradation boundary are shown in Fig. 11 and Fig. 12. According to the above comparative tables and figures, compared with the other models, M_0 is superior not only in predicting the deterministic degradation, but also in the uncertainty quantification. Additionally, the uncertainty quantification of M_0 and M_1 is considerably superior to that

of models M_2 and M_3 , demonstrating the necessity of considering the long-range dependence in the degradation process.

Table 7 Quantitative indices of the microwave case under all stress levels.

Model	\overline{ER}	\overline{ER}^U	\overline{ER}^L
M_0	0.1335	0.9389	3.7036
M_1	0.1490	1.1209	3.8215
M_2	0.1429	2.3264	12.3555
M_3	0.1849	2.4501	11.3810

Note: The bolded results depict the best ones.

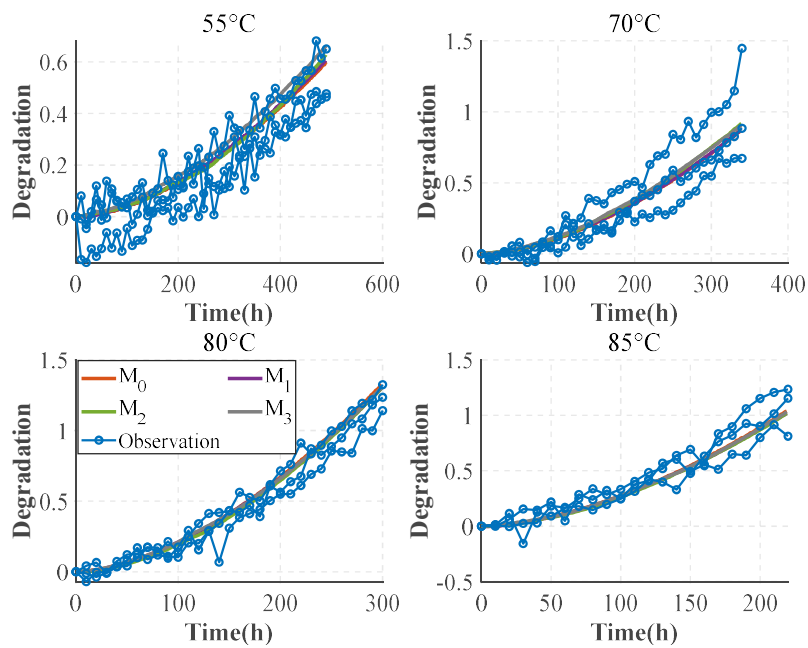


Fig. 11 Prediction for the deterministic degradation trend under all stress levels.

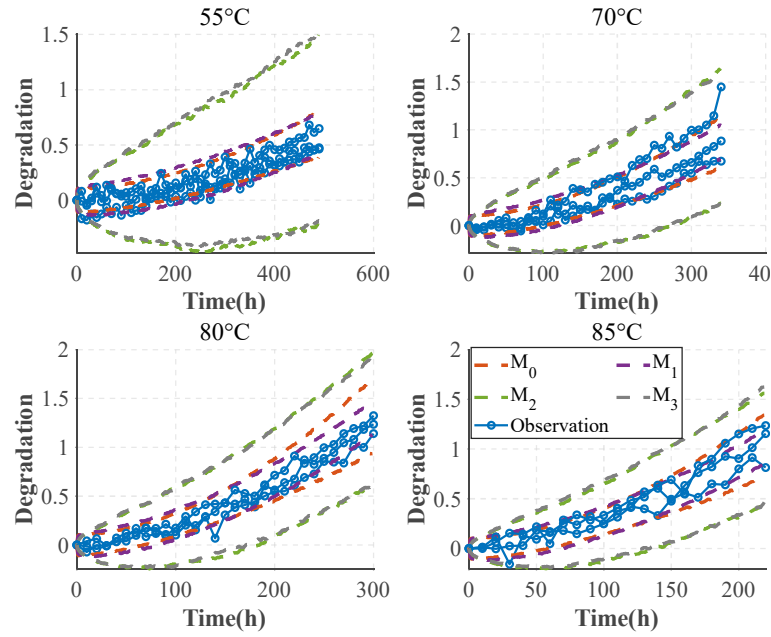


Fig. 12 Prediction for the degradation boundary under all stress levels.

5.3.2 Comparison of model extrapolation

In this subsection, we develop the cross-validation scheme [40] shown in Table 8 to explore the extrapolation capability of the four ADT models. The quantitative indices of cross-validation 1 and 2 are listed in Table 9 and Table 10. The visualization results are shown in Fig. 13 and Fig. 14. From the above comparative tables and figures, the following results can be obtained:

- According to Table 9 and Table 10, no matter for the cross-validation 1 or 2, the predictions of deterministic degradation trend based on M_0 are both the best ones by great superiority. In terms of uncertainty quantification, the upper and lower boundary predictions based on M_0 are both the best for cross-validation 2, while the lower boundary predictions based on M_0 are worse than those of M_1 for cross-validation 1. Overall, model M_0 has a superior capacity for uncertainty quantification.
- From Fig. 13 and Fig. 14, no matter for the cross-validation 1 or 2, M_0 best describes the deterministic degradation trend and envelopes the real data, proving the superiority of the model M_0 .
- By analyzing the predictions of the four ADT models for two cross-validations, we can deduce that M_0 is more suitable for lifetime and reliability inference under the normal stress level in this case.

Table 8 Plans of cross-validation

Projects	Training data	Testing data
Cross-validation 1	The data under all stress levels except the lowest stress level	The data under the lowest stress level (55°C)
Cross-validation 2	The data under all stress levels except the highest stress level	The data under the highest stress level (85°C)

Table 9 Quantitative indices of the microwave case for the cross-validation 1.

Model	\overline{ER}_1	\overline{ER}_1^U	\overline{ER}_1^L
M_0	0.2937	0.7971	3.3203
M_1	0.4637	1.2940	1.3456
M_2	0.4973	3.2261	27.1602
M_3	0.3621	3.2290	28.5961

Note: The bolded results depict the best ones.

Table 10 Quantitative indices of the microwave case for the cross-validation 2.

Model	\overline{ER}_4	\overline{ER}_4^U	\overline{ER}_4^L
M_0	0.1249	0.4198	9.8124
M_1	0.2167	0.4468	9.9591
M_2	0.1617	0.8326	11.8889
M_3	0.2153	0.7809	12.5949

Note: The bolded results depict the best ones.

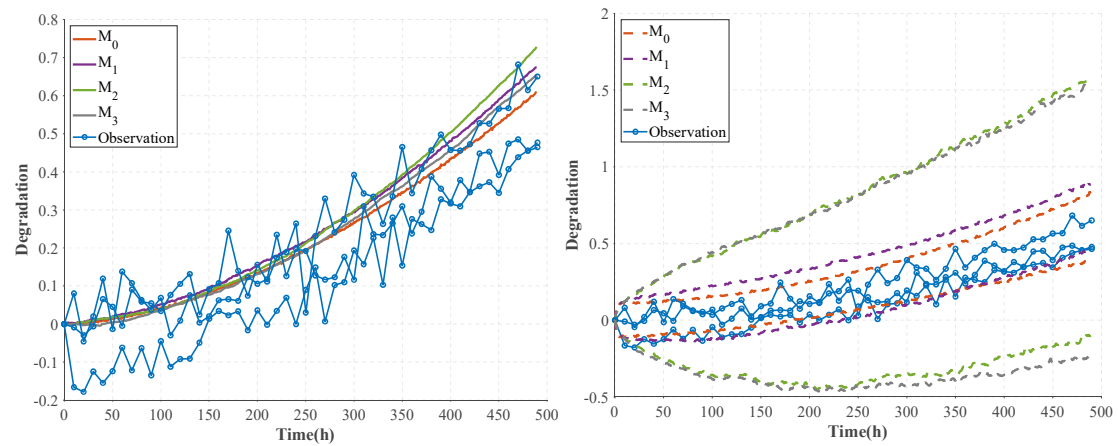


Fig. 13 Prediction for the cross-validation 1: (a) deterministic degradation trend (b) degradation boundary.

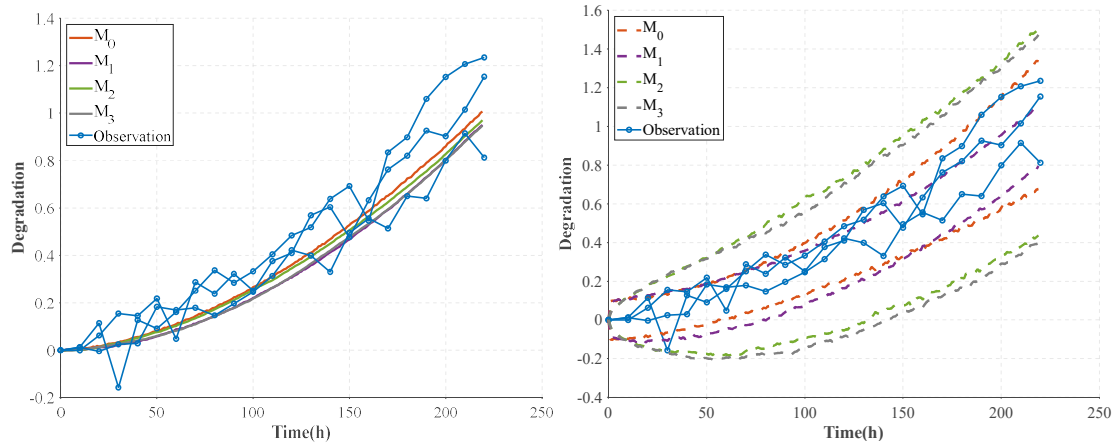


Fig. 14 Prediction for the cross-validation 2: (a) deterministic degradation trend (b) degradation boundary.

6 Conclusion

This paper aims to address the problems of lacking an ADT model considering both the long-range dependence and unit-to-unit variability. The following conclusions can be drawn from this paper:

- This paper proposes an improved non-Markovian ADT model considering both the long-range dependence and unit-to-unit variability. The long-range dependence is quantified by the Hurst exponent in the FBM and the unit-to-unit variability is clearly analyzed and quantified in the degradation rate function. Then, the lifetime distribution and reliability are calculated by the MC method. Besides, a novel statistical inference method based on the EM algorithm is proposed to ensure the maximization of the overall likelihood function.
- The results of the simulation case illustrate that the parameter estimations of the proposed statistical inference method are more accurate than those of the two-step MLE method, especially when degradation has the property of long-range dependence and the number of measurements is small. Moreover, without considering unit-to-unit variability, wrong degradation law will be deduced.
- A microwave case is utilized to verify the effectiveness of the proposed methodology. Results show that ADT models considering long-range dependence are superior in uncertainty quantification. Besides, the proposed model gives superior predictions in both deterministic degradation trends and uncertainty quantification compared to the existing ADT models.

Beyond the work of this study, there are other issues that merit future research. For example, we only focus on modeling constant-stress ADT data in this work. Constructing an ADT model considering long-range dependence for the step-stress ADT data is an interesting topic and worth further research.

Acknowledgements

This work was supported by the National Natural Science Foundation of China [grant number 51775020], the Science Challenge Project [grant number. TZ2018007], the National Natural Science Foundation of China [grant numbers 62073009].

References

- [1]Charki A., Laronde R., Bigaud D. Accelerated degradation testing of a photovoltaic module. *Journal of photonics for energy*. 2013, 3(1): 033099-033099.
- [2]Santini T., Morand S., Fouladirad M., et al. Accelerated degradation data of SiC MOSFETs for lifetime and Remaining Useful Life assessment. *Microelectronics Reliability*. 2014, 54(9): 1718-1723.
- [3]Yan W., Riahi H., Benzarti K., et al. Durability and Reliability Estimation of Flax Fiber Reinforced Composites Using Tweedie Exponential Dispersion Degradation Process. *Mathematical Problems in Engineering*. 2021, 2021: 6629637.
- [4]Li X.-Y., Wu J.-P., Liu L., et al. Modeling accelerated degradation data based on the uncertain process. *IEEE Transactions on Fuzzy Systems*. 2018, 27(8): 1532-1542.
- [5]Liu Z., Li X., Kang R. Uncertain differential equation based accelerated degradation modeling. *Reliability Engineering and System Safety*. 2022, 225.
- [6]Wang C., Liu J., Yang Q., et al. Recoverability effects on reliability assessment for accelerated degradation testing. *IIEE Transactions*. 2023, 55(7): 698-710.
- [7]Zhang H., Zhou D., Chen M., et al. FBM-Based Remaining Useful Life Prediction for Degradation Processes With Long-Range Dependence and Multiple Modes. *IEEE Transactions on Reliability*. 2018.
- [8]Guérin T., Levernier N., Bénichou O., et al. Mean first-passage times of non-Markovian random walkers in confinement. *Nature*. 2016, 534(7607): 356-359.
- [9]Giorgio M., Pulcini G. A new age- and state-dependent degradation process with possibly negative increments. *Quality and Reliability Engineering International*. 2019, 35(5): 1476-1501.
- [10]Giorgio M., Guida M., Pulcini G. A new class of Markovian processes for deteriorating units with state dependent increments and covariates. *IEEE Transactions on Reliability*. 2015, 64(2): 562-578.
- [11]Peng W., Zhu S.-P., Shen L. The transformed inverse Gaussian process as an age-and state-dependent degradation model. *Applied Mathematical Modelling*. 2019, 75: 837-852.
- [12]Duan F., Wang G. Bayesian analysis for the transformed exponential dispersion process with random effects. *Reliability Engineering & System Safety*. 2022, 217: 108104.
- [13]Sottinen T. Fractional Brownian motion, random walks and binary market models. *Finance and Stochastics*. 2001, 5(3): 343-355.
- [14]Burnecki K., Kepten E., Janczura J., et al. Universal algorithm for identification of fractional Brownian motion. A case of telomere subdiffusion. *Biophysical Journal*. 2012, 103(9): 1839-1847.
- [15]Zhang H., Chen M., Shang J., et al. Stochastic process-based degradation modeling and RUL prediction: from Brownian motion to fractional Brownian motion. *Science China Information Sciences*. 2021, 64(7).
- [16]Xi X., Chen M., Zhou D. Remaining Useful Life Prediction for Degradation Processes with Memory Effects. *IEEE Transactions on Reliability*. 2017, 66(3): 751-760.
- [17]Xi X., Chen M., Zhang H., et al. An improved non-Markovian degradation model with long-term dependency and item-to-item uncertainty. *Mechanical Systems and Signal Processing*. 2018, 105: 467-480.
- [18]Shao Y., Si W. Degradation Modeling With Long-Term Memory Considering Measurement Errors. *IEEE Transactions on Reliability*. 2021.
- [19]Xi X., Zhou D., Chen M., et al. Remaining useful life prediction for multivariable stochastic

degradation systems with non-Markovian diffusion processes. *Quality and Reliability Engineering International*. 2020, 36(4): 1402-1421.

[20]Si W., Shao Y., Wei W. Accelerated Degradation Testing with Long-Term Memory Effects. *IEEE Transactions on Reliability*. 2020, 69(4): 1254-1266.

[21]Li N., Lei Y., Yan T., et al. A Wiener-process-model-based method for remaining useful life prediction considering unit-to-unit variability. *IEEE Transactions on Industrial Electronics*. 2018, 66(3): 2092-2101.

[22]Hou Y., Du Y., Peng Y., et al. An Improved Random Effects Wiener Process Accelerated Degradation Test Model for Lithium-Ion Battery. *IEEE Transactions on Instrumentation and Measurement*. 2021, 70.

[23]Jiang P. Statistical Inference of Wiener Constant-Stress Accelerated Degradation Model with Random Effects. *Mathematics*. 2022, 10(16): 2863.

[24]Mandelbrot B.B., Van Ness J.W. Fractional Brownian motions, fractional noises and applications. *SIAM Review*. 1968, 10(4): 422-437.

[25]Liu L., Li X., Sun F., et al. A general accelerated degradation model based on the wiener process. *Materials*. 2016, 9(12).

[26]Li X.Y., Chen D.Y., Wu J.P., et al. 3-Dimensional general ADT modeling and analysis: Considering epistemic uncertainties in unit, time and stress dimension. *Reliability Engineering and System Safety*. 2022, 225.

[27]Przondziono R., Timothy J.J., Weise F., et al. Degradation in concrete structures due to cyclic loading and its effect on transport processes—Experiments and modeling. *Structural Concrete*. 2017, 18(4): 519-527.

[28]Escobar L.A., Meeker W.Q. A review of accelerated test models. *Statistical Science*. 2006. 552-577.

[29]Ye Z.S., Chen L.P., Tang L.C., et al. Accelerated degradation test planning using the inverse gaussian process. *IEEE Transactions on Reliability*. 2014, 63(3): 750-763.

[30]Ye X., Hu Y., Zheng B., et al. A new class of multi-stress acceleration models with interaction effects and its extension to accelerated degradation modelling. *Reliability Engineering and System Safety*. 2022, 228.

[31]Wu J.-P., Kang R., Li X.-Y. Uncertain accelerated degradation modeling and analysis considering epistemic uncertainties in time and unit dimension. *Reliability Engineering and System Safety*. 2020, 201: 106967.

[32]Tang S., Guo X., Yu C., et al. Accelerated degradation tests modeling based on the nonlinear wiener process with random effects. *Mathematical Problems in Engineering*. 2014, 2014.

[33]Liao C.M., Tseng S.T. Optimal design for step-stress accelerated degradation tests. *IEEE Transactions on Reliability*. 2006, 55(1): 59-66.

[34]Wood A.T., Chan G. Simulation of stationary Gaussian processes in $[0, 1]$ d. *Journal of computational and graphical statistics*. 1994, 3(4): 409-432.

[35]Dempster A.P., Laird N.M., Rubin D.B. Maximum likelihood from incomplete data via the EM algorithm. *Journal of the royal statistical society: series B (methodological)*. 1977, 39(1): 1-22.

[36]Li H., Pan D., Chen C.L.P. Reliability modeling and life estimation using an expectation

maximization based wiener degradation model for momentum wheels. *IEEE Transactions on Cybernetics*. 2015, 45(5): 969-977.

[37]Pan D., Wei Y., Fang H., et al. A reliability estimation approach via Wiener degradation model with measurement errors. *Applied Mathematics and Computation*. 2018, 320: 131-141.

[38]Cavanaugh J.E., Neath A.A. The Akaike information criterion: Background, derivation, properties, application, interpretation, and refinements. *Wiley Interdisciplinary Reviews: Computational Statistics*. 2019, 11(3): e1460.

[39]Sun F., Fu F., Liao H., et al. Analysis of multivariate dependent accelerated degradation data using a random-effect general Wiener process and D-vine Copula. *Reliability Engineering & System Safety*. 2020, 204: 107168.

[40]Shao J. Linear model selection by cross-validation. *Journal of the American Statistical Association*. 1993, 88(422): 486-494.